Journal of the Korean Chemical Society
1996, Vol. 40, No. 12
Printed in the Republic of Korea

역광전자분광기의 제작 및 그 응용

金鉦原 · 金世勳
한국과학기술원 화학과
(1996. 9. 10 접수)

Construction of Inverse Photoemission Spectrometer and Its Application

Jeong Won Kim and Sehun Kim
Department of Chemistry and Center for Molecular Science, Korea Advanced Institute of Science & Technology, Taejon 305-701, Korea
(Received September 10, 1996)

요 약. 고체표면의 비점유 전자에너지 상태를 연구하고자 역광전자분광기를 제작하고 시험하였다. 이 분광기는 초고진공 챔버속에 저에너지 전자총과 광검출기로 구성되어 있다. 전자총은 궤도 시뮬레이션과 전류 측정을 통해 좋은 집속도와 높은 전류밀도를 가지고 있음을 알 수 있었다. 이 분광기의 전체적인 분해능은 0.74 eV이고, 광검출기의 감도는 약 10 counts/sec·μA이다. 하나의 결과로서 Ge(111) 시료의 역광전자분광 스펙트럼은 이론적인 계산결과와 잘 일치하였다.

ABSTRACT. An inverse photoemission spectrometer has been built and tested to study the unoccupied electron energy states of solid surfaces. It consists of a low energy electron gun and a band pass photon detector in an ultra-high vacuum chamber. The electron ray tracing simulation and current measurement of the electron gun show a good focus and a high flux of electron current. The overall resolution of the spectrometer is 0.74 eV and the sensitivity of the photon detector is about 10 counts/sec·μA. As a test experiment, the inverse photoemission spectra of a Ge(111) sample is in good agreement with the theoretical result.

INTRODUCTION

One of the major aims of surface scientists is to understand the electronic band structures of solid surfaces because the electronic band structures are an important basis characterizing a given solid surface. Using the photoionization phenomena is a conventional method to study these properties of solids. From the direct photoemission process we obtain the informations of the occupied states, but little about the unoccupied states. Inverse Photoemission Spectroscopy (IPS) has been developed as a technique for probing the unoccupied electronic states in solids.[1,2] The direct access of the unoccupied electronic states of a solid surface plays an important role in the study of the surface chemical bonds.[3] Most actively studied topics are the surface states associated with the long-range nature of the image potential,[4] the conduction band and dangling bond states of semiconductors, and the electronic structural changes due to adsorption and metal-semiconductor contacts. In addition to the momentum resolved IPS, using a spin-polarized electron gun, one obtains spin-dependant spectra, and it is possible to investigate the magnetic properties of surfaces and thin films.[5] IPS is nearly ideal in the sense that it is capable of determining all the quantum numbers of an electron of a solid and at a surface, which is thought to be complementary to ultraviolet photoemission spectroscopy (UPS). Such a complete measurement is rather difficult in practice, but the technical problems have been eased during the last decade and

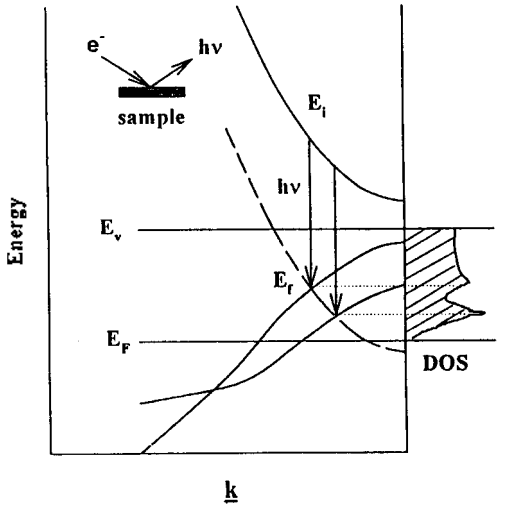

Fig. 1. Schematic of the inverse photoemission process and its energy diagram.

a wealth of experimental information has been accumulated. In this note, we describe a details of a home-made IPS system and show the possibility of the IPS applications.

Fig. 1 represents an inverse photoemission process and its energy diagram. General principles of IPS are available in many articles.[6] Electrons impinging on a solid surface with the energy E_i decay via radiative transitions to other low lying unoccupied electronic bands (for example, conduction band) of energy E_f above the Fermi energy level E_F. *Fig.* 1 shows the case where two (or more) different radiative transitions from the same initial band are possible as is called an isochromat. Suppose the electrons impinging on the sample have a well-defined energy E_i, we obtain the quantum energy of the emitted photons $h\nu$ corresponding to E_i-E_f.

ELECTRON GUN

IPS spectrometer consists of a low energy electron source and a band-pass photon detector in an ultra-high vacuum (UHV) system. The use of low energy electrons has many advantages over Bremsstrahlung isochromatic spectroscopy (BIS) which uses a high energy electron source. It cuts the radiation damage enormously and obtains a

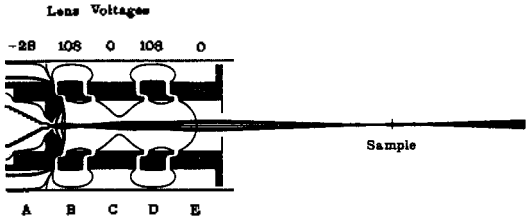

Fig. 2. A cross-sectional view of the electron gun and the simulation of its ray tracing at the electron beam voltage of 20 eV.

monolayer sensitivity due to the shorter electron mean free path. Another important advantage of low electron energies is the fact that the momentum information of the electronic states can be probed using a simple conservation law. At several keV energy of electron, it is much harder to keep the momentum defined within a fraction of the Brillouin zone (*i.e.*, the unit cell in k-space with a typical radial dimension of $Å^{-1}$). Also, the enhanced thermal scattering and the finite momentum of the photons blur the momentum balance in the high-energy regime.

General schemes for the electron gun design have been discussed previously.[7~10] These electron guns had a high current and a moderate angular resolution, but some types of these electron guns were critically dependent upon the electrode shaping. The electron gun for IPS must have a good energy and angular resolution and also should keep delivering a high current electron beam because of low cross section for the production of photons. In order to meet these needs, we chose an analogy of the Erdman and Zipf's model.[8] *Fig.* 2 represents a cross-sectional view of the gun and the simulation of its ray tracing at the electron energy of 20 eV. The electron gun consists of a filament, a filament mounting block and grid (A), three-element Einzel lens (B, C, D), and a final ground plate (E). In order to optimize the electron beam current we have modified the grid, so called extractor with a cone shape aperture. All the elements are cylindrically symmetric and made of stainless steel 304, and then electrochemically gold-plated to minimize the space charge effect. Each adjacent element is electrically separated by

three 2.36 mm sapphire balls (Kimball Physics Inc., Saph-BA-B) and all elements are held tightly by four 1/16" screws. The assembly is mounted on the 2.75 CF-Flange, and then magnetically shielded by a μ-metal tube (Hamamatsu, E989-03). The entire assembly can make a precise, strong and stable mechanical structure with each element-separation of 1.2 mm, and total length of 51 mm. The assembly and the mounting geometry make the maximum angular divergence of 4°. A thoria-coated tungsten wire filament ($\phi=0.20$ mm) was used as the electron emitter. The operation temperature of the filament is 1925 K, and its thermal energy spread is about 0.43 eV which is better than that of a bare tungsten filament. Recently people have used a BaO dispenser cathode. The operation temperature of the BaO cathode is 1100~1300 K, and the energy spread is about 0.22 eV producing a better resolution. However, there are some disadvantages that the BaO cathode are gradually degraded and has a shorter life time.

Fig. 2 shows the simulations of 20 trajectories obtained by using SIMION program[11] varying the starting electron energy, position, and angle for our electron gun. The operating beam-voltage of the electron gun spans usually from 5 to 25 eV. The simulation of ray tracing at 20 eV is shown here. The ratio between lens voltages is the same over the whole energy range. The Wehnelt voltage to the gun element A (grid) is sensitive to the beam current until a proper voltage ratio reaches. The anode voltage (B and D) needs not be so accurate but affects seriously the focal length. The higher the voltage, the shorter the focal length. The Wehnelt voltage and the first anode voltage together determine the electron emission current. Before the signal counting, the performance of the electron gun was checked. The filament current was 4.0 A and more than 10 μA-beam current was detected at 20 eV electron energy. The beam focusing was tested at an elevated energy of about 150 eV on the phosphor-covered target. The spot size was less than 2 mm diameter. Each lens voltage was optimized in the way of maximizing the electron beam current.

PHOTON DETECTOR

Basically, there are two approaches for building a photon detector. One is a tunable photon energy detector using a grating monochromator.[12] However, this is not so popular, because it is usually complex and suffers from very low counting rate because of its small acceptance angle. The other is a fixed energy detector, so called isochromatic mode, which can accept a large solid angle but sacrifices tunability. One of the most common detector is the Geiger-Müller (GM) counter working as a band-pass photon detector between the photoionization threshold of iodine and optical window cutoff-energy.[13] The resolution of this GM counter is usually 0.7~0.8 eV dependent upon the used window.[14] But, the GM counter has some difficulties in iodine gas sealing and baking in the UHV chamber. To resolve these problems, in this work we used a photomultiplier detector which consists of a modified CuBe cathode electron multiplier (Thorn EMI model, EM132) and a CaF_2 entrance window (International Crystal Lab., 2×20 mm disc).[15] The optical transmission of the CaF_2 and the spectral photoelectron yield of CuBe cathode operate as low and high pass filter respectively. The diagram of the photon detecter is represented in *Fig.* 3. The array of 12 dynodes is connected with 1 MΩ resistors and produces about 1.5×10^6 gain. In front of the window, there is a fine W-mesh to avoid the window charging and to shield the anode potential. The 2.5 kV bias voltage was typically used. It was reported that the maximum sensitivity of the detector lay at 9.8 eV and broadening was 0.6 eV.[15] In this geometry, the solid

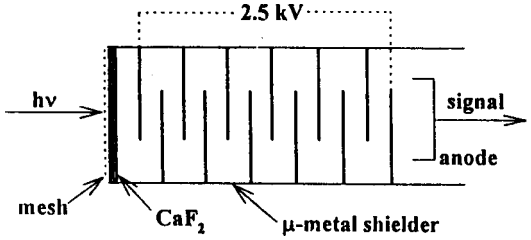

Fig. 3. A diagram of the photon detector using a CaF_2 window and electron multiplier. An array of 12 CuBe dynodes is connected by 1 MΩ resistors.

angle of the detector is 0.08 sr since the first CuBe cathode area is 54 mm^2 and the distance from the center is about 40 mm. The whole system is shielded in a μ-metal tube and mounted on a 2.75″ CF-Flange. In comparison with the GM counter, the detection efficiency of this detector is said to be comparable, and the energy resolution slightly better. Additionally, it has a higher gain stability, practically no dead time, and offers a good UHV compatibility. In the recent study, we are trying the SrF_2 window at the entrance of the photon detector to change the short-wave transmission limit from 1220 $Å^{-1}$ (about 10.2 eV) to 1280 $Å^{-1}$ (9.7 eV) to make a better resolution.

The overall energy resolution of the IPS spectrometer is given by the thermal energy spread of the electron gun and the bandwidth of the photon detector. The resolution is approximately $\Delta E=\sqrt{0.43^2+0.6^2}=0.74$ eV, in which the thoria-coated tungsten cathode and the electron multiplier with CaF_2 window are used. It can be improved to ~0.3 eV if we modified the spectrometer with a SrF_2 window and a BaO cathode.

IP SPECTRA OF Ge

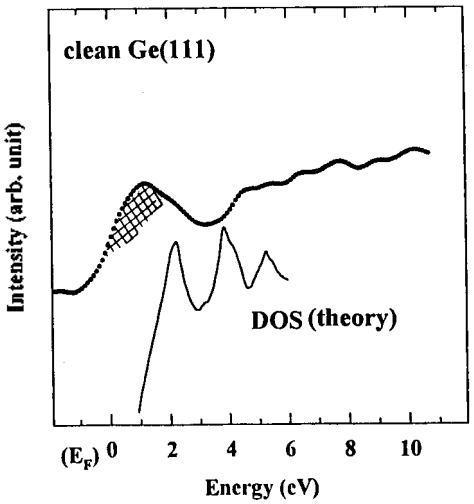

Fig. 4. Isochromat for clean Ge(111) surface. The solid line is the theoretical calculation of unoccupied density of states of Ge.[16] The hatched area is the surface density of states of Ge(111).

Fig. 4 represents the IP spectra for the clean Ge(111) surface. The Ge(111) single crystal sample was cleaned by repeated cycles of Ar^+-sputtering (800 eV) and annealing (900 K). *Fig.* 4 shows the data subtracting a exponential background increase with electron energy. The solid line is the theoretical data of the bulk density of unoccupied states of Ge,[16] which is in good agreement with the experimental data, considering the instrumental resolution of 0.74 eV. The hatched area near the E_F is the surface density of states due to adatoms of Ge(111)-c(2×8).[5(d)] The spectrum was obtained with 16 seconds duration for each data point. The counting rates are 23 sec^{-1} at 10 eV, and 63 sec^{-1} at 15 eV of electron energy. The sensitivity of the system is comparable to Denninger *et al.*'s experiment,[13] 1.6×10^7 counts/C (=16 counts/sec·μA) using GM counter and the same CaF_2 window as ours. However, this value is lower than theoretically suggested, $\sim3\times10^2$ photons/sec·0.08 sr[6(b)] because it is not corrected for the transmission of the CaF_2 window and W-mesh or the loss of pulses below the discriminator threshold. To get higher counting rate, a larger acceptance angle is favorable. Since the solid angle is limited by the size of the first CuBe cathode in an electron multiplier, using a larger cathode in the electron multiplier or UV mirror is the way to increase the solid angle. The photon detector with a GM counter with a SrF_2 window of larger diameter might satisfy all of these conditions.

SUMMARY

In summary, we constructed the IPS spectrometer and tested its performance. We used the modified electron gun with the thoria-coated tungsten filament and the electron multiplier with the CaF_2 window as a band-pass photon detector. The electron gun has a good focus and delivers a favorable current, about 10 μA at electron energy 20 eV. The overall resolution is 0.74 eV and the sensitivity of the photon counter is about 10 counts/sec·μA in our IPS system. As a test experiment, we obtained the unoccupied density of states of a clean Ge(111) sample, which is in agreement with

the data of the theoretical calculation and surface density of states.

Acknowledgement. This work was supported by the Center for Molecular Science and KAIST. We thank Dr. B. Kim for helpful discussion.

REFERENCES

1. Fuggle, J. C.; Inglesfield, J. E. *Unoccupied Electronic States*; Springer-Verlag: New York, U. S. A., 1992.
2. Dose, V. *Appl. Phys.* **1977**, *14*, 117.
3. Goldmann, A.; Donath, M.; Altmann, W.; Dose, V. *Phys. Rev. B* **1985**, *32*, 837.
4. Johnson, P. D.; Smith, N. V. *Phys. Rev. B* **1983**, *27*, 2527.
5. (a) Ciccacci, F.; Vescovo, E.; Chiaia, G.; De Rossi, S.; Tosca, M. *Rev. Sci. Instrum.* **1992**, *63*, 3333. (b) Donath, M. *Appl. Phys. A* **1989**, *49*, 351.
6. (a) Dose, V. *Surf. Sci. Rep.* **1985**, *5*, 337. (b) Smith, N. V. *Rep. Prog. Phys.* **1988**, *51*, 1227. (c) Borstel, G.; Thörner, G. *Surf. Sci. Rep.* **1987**, *8*, 1. (d) Himpsel, F. J. *Surf. Sci. Rep.* **1990**, *12*, 1. (e) Kim, B. Ph. D thesis, Iowa State Univ., 1990. (f) Suga, S.; Mamatame, H.; Ogawa, S.; Kinoshita, T. 分光研究 **1990**, *39*, 2. (g) Himpsel, F. J.; Fauster, Th. *J. Vac. Sci. Technol. A* **1984**, *2*, 815. (h) Pendry, J. B. *J. Phys. C: Solid State Phys.* **1981**, *14*, 1381.
7. Simpson, J.; Kuyatt, C. E. *Rev. Sci. Instrum.* **1963**, *34*, 265.
8. Erdman, P. W.; Zipf, E. O. Rev. Sci. Instrum. **1982**, *53*, 225.
9. Stoffel, N. G.; Johnson, P. D. *Nucl. Instrum. Meth. Phys. Res. A* **1985**, *234*, 230.
10. Hillebrecht, F. U.; Keppels, J.; Otto, R. *Rev. Sci. Instrum.* **1987**, *58*, 776.
11. Dahl, D. A.; Delmore, J. E. *SIMION PC/PS2 ver. 4.0*, EG&G Idaho Inc., 1988.
12. (a) Fuaster, Th.; Himpsel, F. J.; Donelon, J. J.; Mark, A. *Rev. Sci. Instrum.* **1983**, *54*, 68. (b) Fuaster, Th.; Straub, D.; Donelon, J. J.; Grimm, D.; Marx, A.; Himpsel, F. J. *ibid.* **1985**, *56*, 1212. (c) Royer W. A.; Smith, N. V. *ibid.* **1988**, *59*, 737.
13. Denninger, G.; Dose, V.; Scheidt, H. *Appl. Phys.* **1979**, *18*, 375.
14. Dose, V.; Fauster Th.; Schneider, R. *Appl. Phys. A* **1986**, *40*, 203.
15. Babbe, N.; Drube, W.; Schäfer, I.; Skibowski, M. *J. Phys. E: Sci. Instrum.* **1985**, *18*, 158.
16. Chelikowsky, J. R.; Cohen, M. L. *Phys. Rev. B* **1976**, *14*, 556.